

## Hot-injection Polyol 공정에 의해 제조된 $\text{Fe}_3\text{O}_4$ 나노입자의 Hyperthermia 특성

이성노 · 고태준 · 심인보\*

국민대학교 물리학과, 서울시 성북구 정릉동 861-1, 136-702

심현주

한국외국어대학교부속 용인외국어고등학교, 경기 용인시 처인구 모현면 외대로54번길 50, 449-854

(2014년 2월 14일 받음, 2014년 4월 14일 최종수정본 받음, 2014년 4월 16일 게재확정)

$\text{Fe}_3\text{O}_4$  나노입자는 hot-injection 제조법에 의해 제조되었으며 반응물질의 injection time에 변화를 주었다. 격자구조는 x-ray diffraction(XRD) 측정을 통해 Fd-3m 공간군을 갖는 cubic inverse spinel 구조로 분석되었으며,  $\text{Fe}_3\text{O}_4$  나노입자의 형상은 high-resolution transmission electron microscope(HR-TEM)으로 분석하였다. 반응물질을 각각 0.5분, 60분인 켄션 시 각각 7.63 nm, 21.73 nm의  $\text{Fe}_3\text{O}_4$  나노입자 사이즈를 얻을 수 있었다.  $\text{Fe}_3\text{O}_4$  나노입자의 자기적 특성은 다양한 온도에서 vibrating sample magnetometer(VSM)과 Mössbauer spectroscopy로 측정하였으며, hyperthermia 측정을 통해 반응물질의 injection time이 60분일 때 50 kHz의 250 Oe에서  $\text{Fe}_3\text{O}_4$  나노입자 파우더의 온도가 약 120 °C임을 관측할 수 있었다.

주제어 :  $\text{Fe}_3\text{O}_4$  nanoparticle, Mössbauer spectroscopy, hyperthermia

## Hyperthermia Properties of $\text{Fe}_3\text{O}_4$ Nanoparticle Synthesized by Hot-injection Polyol Process

Seong Noh Lee, Taejoon Kouh, and In-Bo Shim\*

Department of Physics, Kookmin University, Seoul 136-702, Korea

Hyun Ju Shim

Hankuk Academy of Foreign Studies, Gyeonggi-do 449-854, Korea

(Received 14 February 2014, Received 14 April 2014, Accepted 16 April 2014)

The  $\text{Fe}_3\text{O}_4$  nanoparticle was synthesized by the hot-injection method while varying the injection time of the precursor solution. The crystal structure was determined to be cubic inverse spinel with space group of Fd-3m based on X-ray diffraction (XRD) measurements and the morphology of the prepared  $\text{Fe}_3\text{O}_4$  nanoparticle was studied with a high-resolution transmission electron microscope (HR-TEM). When the precursor solution was injected for 0.5 min, the size of the  $\text{Fe}_3\text{O}_4$  nanoparticle was 7.63 nm, while the size of the obtained particle was 21.27 nm with the injection time of 60 min. The magnetic properties of the prepared  $\text{Fe}_3\text{O}_4$  nanoparticle were investigated by both vibrating sample magnetometer (VSM) and  $^{57}\text{Co}$  Mössbauer spectroscopy at various temperatures. From the hyperthermia measurement, we observed that the temperature of the  $\text{Fe}_3\text{O}_4$  nanoparticle powder reached around 120 °C under 250 Oe at 50 kHz, when the injection time of the precursor solution was 60 min.

Keywords :  $\text{Fe}_3\text{O}_4$  nanoparticle, Mössbauer spectroscopy, hyperthermia

## I. Introduction

Ferrite materials, having excellent electromagnetic properties such as high electric resistivity [1], high magnetic permeability [2], and electromagnetic wave absorption characteristics [3], have been studied extensively in the past decade. Also, the ferrites have been widely used in various industrial applications such as a magnetic sensor, biocatalyst, and waste water treatment [4].

Among the various forms of the ferrite materials, the ferrite nanoparticle with spinel structure have been used in data storage and biomedical applications such as media recording device [5], drug delivery [6], hyperthermia treatment [7] and magnetic resonance imaging [8], due to its unique physical and chemical properties depending on the particle size. Especially, the magnetite ( $\text{Fe}_3\text{O}_4$ ) has been investigated as a material for the hyperthermia treatment due to its non-toxicity and high stability with high Curie temperature of 858 K [9], suitable for the biomedical applications.

In this study, we have prepared  $\text{Fe}_3\text{O}_4$  nanoparticles with various shapes via hot-injection method [10] and investigated their crystal structure, microstructure and electromagnetic properties. We have also measured the hyperthermia properties of  $\text{Fe}_3\text{O}_4$  nanoparticle under external ac magnetic field.

## II. Experiments

$\text{Fe}_3\text{O}_4$  nanoparticle was synthesized by the modified hot-injection method with 0.04 ml of oleic acid ( $\text{C}_{17}\text{H}_{33}\text{COOH}$ , 90 %), 0.04 ml of oleylamine ( $\text{C}_{18}\text{H}_{35}\text{NH}_2$ , 70 %), and 1.31 g of 1, 2-tetradecanediol (90 %), mixed into 15 ml of benzyl ether ( $\text{C}_{14}\text{H}_{12}\text{O}$ , 98 %) as reaction solution. The reaction solution was heated to 120 °C in vacuum and dehydrated at 120 °C for 1 h. Also, 0.424 g of iron(III) acetylacetonate ( $\text{Fe}(\text{acac})_3$ , 99.9 %) was dissolved into 5 ml of benzyl ether ( $\text{C}_{14}\text{H}_{12}\text{O}$ , 98 %) as precursor solution. The reaction solution was again heated to 290 °C at a rate of 10 °C/min under Ar gas and the precursor solution was injected for 0.5 and 60 min. Then, this prepared solution was kept at 290 °C for 2 h to form nanoparticles and cooled down to room temperature. The synthesized  $\text{Fe}_3\text{O}_4$  nanoparticles from the solution were collected via centrifugal process, followed by washing with ethanol and hexane. To determine the crystal structure and the lattice constant as well as the morphology of  $\text{Fe}_3\text{O}_4$  nanoparticle, XRD and HR-TEM measurements were carried out. The magnetic properties of the nanoparticles were measured by VSM and Mössbauer spectroscopy. Also, the hyperthermia properties of  $\text{Fe}_3\text{O}_4$  nanoparticle powder were characterized under external ac magnetic field.

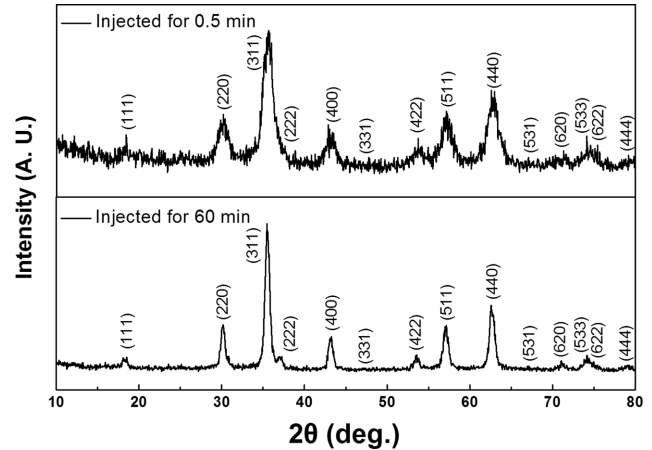


Fig. 1. XRD patterns of  $\text{Fe}_3\text{O}_4$  nanoparticle, synthesized with different precursor injection time.

## III. Results and Discussion

Fig. 1 shows the XRD patterns of  $\text{Fe}_3\text{O}_4$  nanoparticle, synthesized with different precursor injection time. Based on the XRD measurements of  $\text{Fe}_3\text{O}_4$  nanoparticle, the crystal structure was determined to be cubic inverse spinel with space group of  $Fd-3m$ , which is in a good agreement with the standard magnetite data (JCPDS 01-089-3854). The lattice constant  $a_0$  decreased from 8.388 to 8.378 Å with increasing precursor solution injection time. The decreasing lattice constant indicates the densification of crystal structure, associated with the increasing injection time. Also, the peaks in the XRD pattern for injection time of 60 min are sharper than those from the XRD pattern obtained with injection time of 0.5 min, suggesting the changes in nucleation and particle growth with increasing concentration of monomer [11].

The HR-TEM images of  $\text{Fe}_3\text{O}_4$  nanoparticles are shown in Fig. 2 as well as the particle size distribution. From the HR-TEM images, we noticed that when the precursor solution was injected for 0.5 min, the size of nanoparticle was 7.63 nm, while the size was 21.27 nm with the distance between the lattice fringes of 2.3 Å for injection time of 60 min. This suggests the increasing particle size with precursor injection time.

Fig. 3 shows the magnetic hysteresis curves of  $\text{Fe}_3\text{O}_4$  nanoparticle from VSM measurements. The M-H curves show that for the precursor injection time of 0.5 and 60 min, the values of the saturation magnetization ( $M_s$ ) and coercivity ( $H_c$ ) under the applied field of 10 kOe at room temperature are 45.70 emu/g, 5.99 Oe and 64.74 emu/g, 13.50 Oe, respectively. The injection time-dependent crystallization could be one of the possible reasons for increasing saturation magnetization of  $\text{Fe}_3\text{O}_4$  nanoparticle. Also, the small size

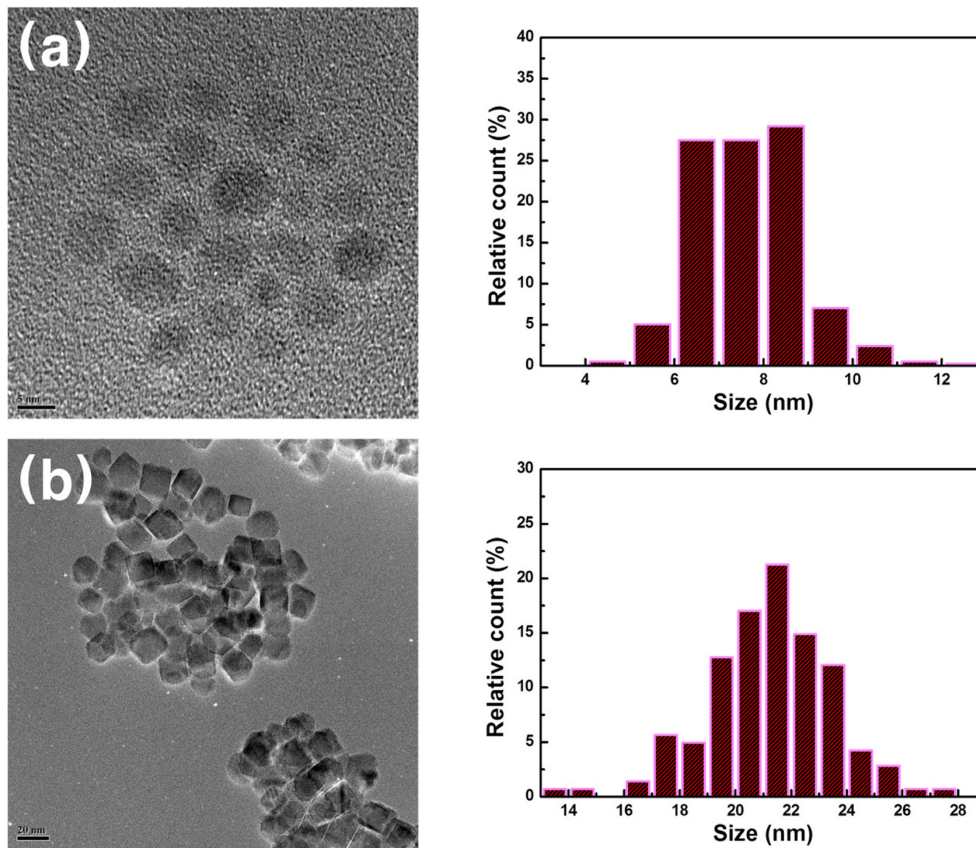


**Fig. 2.** (Color online) HR-TEM images and the particle size distributions of  $\text{Fe}_3\text{O}_4$  nanoparticles synthesized with injection time of (a) 0.5 min and (b) 60 min.

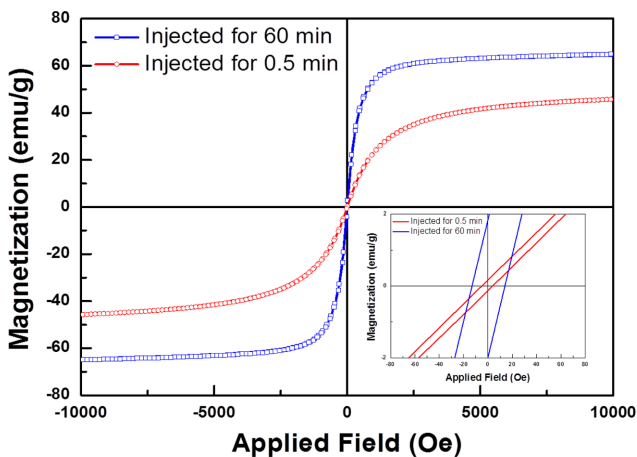


**Fig. 3.** (Color online) Magnetization hysteresis loops of  $\text{Fe}_3\text{O}_4$  nanoparticles measured at 295 K.

of the particle studied here can affect the saturation magnetization via thermal vibration. In addition, due to the geometrical magnetic anisotropy, the coercivity of  $\text{Fe}_3\text{O}_4$  nanoparticle synthesized with injection time of 60 min is larger than that of  $\text{Fe}_3\text{O}_4$  nanoparticle synthesized with injection time of 0.5 min.

In order to investigate the microscopic magnetic properties of  $\text{Fe}_3\text{O}_4$ , Mössbauer spectra of  $\text{Fe}_3\text{O}_4$  nanoparticle were measured at various temperatures from 4.2 to 295 K as shown in Fig. 4. Since  $\text{Fe}_3\text{O}_4$  has an inverse spinel structure with  $[\text{Fe}^{3+}]_A[\text{Fe}^{3+}\text{Fe}^{2+}]_B\text{O}_4$ , we have analyzed Mössbauer spectra as 3-sextet [12]. The resulting Mössbauer parameters from the detailed analysis of the observed spectra are presented in Table I and II, where subscripts A, B1, and B2 denote the tetrahedral ( $\text{Fe}^{3+}$ ), octahedral ( $\text{Fe}^{3+}$ ), and octahedral ( $\text{Fe}^{2+}$ ) sites, respectively. As seen in Fig. 4, while the Mössbauer spectrum at 4.2 K is sharp, the spectra above 220 K shows a broadened central line compared to the paramagnetic central line. This suggests the appearance of superparamagnetism with increasing temperature, which agrees with VSM measurements. The isomer shift values from Mössbauer spectra of  $\text{Fe}_3\text{O}_4$  nanoparticle indicate the presence of both  $\text{Fe}^{3+}$  and  $\text{Fe}^{2+}$  ions, confirming that the prepared nanoparticle is  $\text{Fe}_3\text{O}_4$ . From the Mössbauer measurements, we observe that when the precursor solution is injected for 60 min, the occupancy of  $\text{Fe}^{3+}$  ion is larger than that of  $\text{Fe}^{2+}$  ion at B-site. Also, the difference between the occupancies of cations ( $\text{Fe}^{3+}$ ,  $\text{Fe}^{2+}$ ) at B-site in the  $\text{Fe}_3\text{O}_4$  nanoparticle

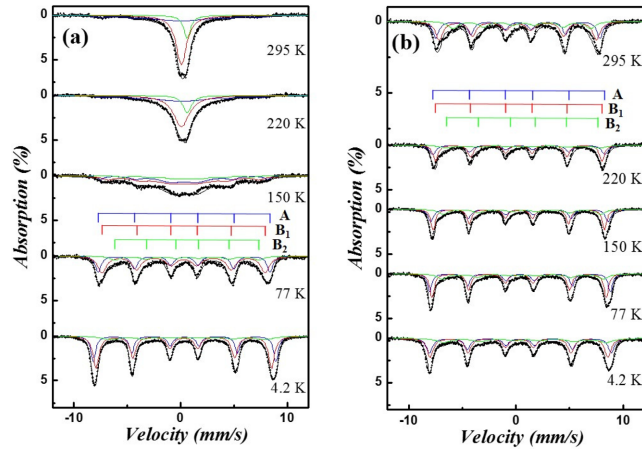
**Table I.** Mössbauer parameters of polyhedral  $\text{Fe}_3\text{O}_4$  nanoparticle at various temperatures.

T (K)	$H_{hf}$ (A) (kOe)	$H_{hf}$ (B <sub>1</sub> ) (kOe)	$H_{hf}$ (B <sub>2</sub> ) (kOe)	$d_A$ (mm/s)	$d_{B_1}$ (mm/s)	$d_{B_2}$ (mm/s)	A (A) (%)	A (B <sub>1</sub> ) (%)	A (B <sub>2</sub> ) (%)
4.2	532	512	450	0.385	0.313	0.664			
77	500	475	419	0.344	0.304	0.610			
150	486	439	374	0.331	0.298	0.601	33.33	51.53	15.13
220	462	-	-	0.121	0.091	0.635			
295	452	-	-	0.019	0.090	0.625			

**Table II.** Mössbauer parameters of cubic  $\text{Fe}_3\text{O}_4$  nanoparticle at various temperatures.

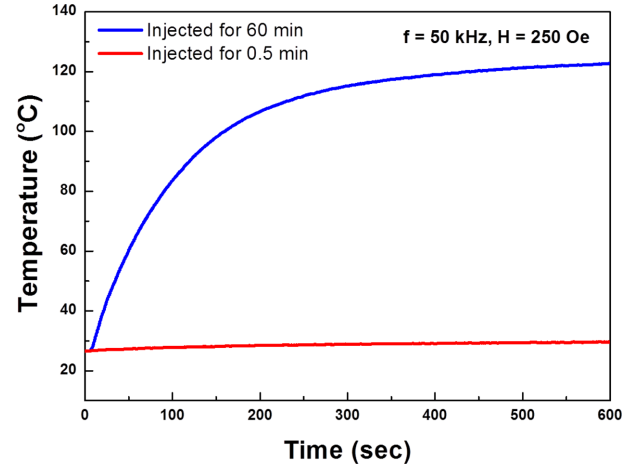
T (K)	$H_{hf}$ (A) (kOe)	$H_{hf}$ (B <sub>1</sub> ) (kOe)	$H_{hf}$ (B <sub>2</sub> ) (kOe)	$d_A$ (mm/s)	$d_{B_1}$ (mm/s)	$d_{B_2}$ (mm/s)	A (A) (%)	A (B <sub>1</sub> ) (%)	A (B <sub>2</sub> ) (%)
4.2	527	516	471	0.399	0.309	0.934			
77	524	505	467	0.375	0.297	0.694			
150	514	497	457	0.338	0.276	0.640	33.33	44.84	21.83
220	499	483	445	0.281	0.261	0.638			
295	477	456	399	0.195	0.320	0.609			

$H_{hf}$  = magnetic hyperfine field,  $\delta$  = isomer shift,  $A$  = ratio of absorption area.

**Fig. 4.** (Color online) Mössbauer spectra of  $\text{Fe}_3\text{O}_4$  nanoparticles synthesized with injection time of (a) 0.5 min and (b) 60 min.

prepared with the injection time of 0.5 min is larger than that in the  $\text{Fe}_3\text{O}_4$  nanoparticle with injection time of 60 min, showing that the occupancy of cation depends on the injection time of precursor solution. We expect that the difference in the occupancy of cation at B-site is possibly originated from the terminated plane or the surface-to-volume ratio.

Fig. 5 shows the hyperthermia properties of  $\text{Fe}_3\text{O}_4$  nanoparticle powder prepared with two different precursor injection times. The self-heating temperature of  $\text{Fe}_3\text{O}_4$  nanoparticles as a function of time was measured under external ac magnetic field of 250 Oe at 50 kHz. We have not observed any changes in the temperature of  $\text{Fe}_3\text{O}_4$  nanoparticle powder synthesized with injection time of 0.5 min. However, the temperature of the nanoparticle powder, synthesized with injection time of 60 min, increased

**Fig. 5.** (Color online) Self-heating temperature of  $\text{Fe}_3\text{O}_4$  nanoparticles under ac magnetic field of 250 Oe at 50 kHz.

above 100 °C after about 200 sec and reached the constant temperature of ~120 °C. Our study suggests that the precursor injection time during the hot-injection process clearly affects the nanoparticle size, which leads to the changes in the total magnetization and conversion of magnetic energy into thermal energy by Neel and Brownian relaxations losses [13].

#### IV. Conclusion

We have synthesized  $\text{Fe}_3\text{O}_4$  nanoparticles via a modified hot-injection method and studied their crystallographic, magnetic and hyperthermia properties using XRD, HR-TEM, VSM and Mössbauer spectroscopy. The nanoparticle studied here has a cubic inverse spinel structure with space group of  $Fd\bar{3}m$ . With the precursor injection time of 0.5 min, polyhedral  $\text{Fe}_3\text{O}_4$  nanoparticle with size of

7.63 nm was synthesized and cubic Fe<sub>3</sub>O<sub>4</sub> nanoparticle with size of 21.27 nm was obtained for the injection time of 60 min. From the Mössbauer spectroscopy measurements, we observed the appearance of superparamagnetism and the large difference between the occupancies of cation (Fe<sup>3+</sup>, Fe<sup>2+</sup>) at B-site in inverse spinel structure of Fe<sub>3</sub>O<sub>4</sub> nanoparticle prepared with injection time of 0.5 min, suggesting that the occupancy of cation depends on the injection time of precursor solution. The self-heating temperature measurements under 250 Oe at 50 kHz show that the temperature of Fe<sub>3</sub>O<sub>4</sub> nanoparticle can be increased up to about 120 °C when the nanoparticle is prepared with injection time of 60 min. Our study indicates that the injection time affects the total magnetization and the conversion of magnetic energy into thermal energy.

### Acknowledgement

This research was supported by Basic Science Research Program and Mid-career Researcher Program through the National Research Foundation of Korea (NRF) grant funded by the Ministry of Education, Science and Technology (MEST) (2010-0022468), and in part by research program of Kookmin University in Korea.

### References

[1] A. Vermaa, T. C. Goel, R. G. Mendiratta, and R. G.

- Gupta, *J. Magn. Magn. Mater.* **192**, 271 (1999).  
 [2] T. Nakamura, *J. Appl. Phys.* **88**, 348 (2000).  
 [3] J. R. Liu, M. Itoh, and K. Machida, *Appl. Phys. Lett.* **83**, 4017 (2003).  
 [4] A. D. Ebner, J. A. Ritter, H. J. Ploehn, R. L. Kochen, and J. D. Navratil, *Separ. Sci. Technol.* **34**, 1277 (1999).  
 [5] Y. Kobayashi, M. Horie, M. Konno, B. Rodríguez-González, and L. M. Liz-Marzán, *J. Phys. Chem. B.* **107**, 7420 (2003).  
 [6] T. J. Yoon, J. S. Kim, B. G. Kim, K. N. Yu, M.-H. Cho, and J.-K. Lee, *Angew. Chem. Int. Ed.* **44**, 1068 (2005).  
 [7] J.-P. Fortin, C. Wilhelm, J. Servais, C. Ménager, J.-C. Bacri, and F. Gazeau, *J. Am. Chem. Soc.* **129**, 2628 (2007).  
 [8] J.-H. Lee, Y.-M. Huh, Y.-W. Jun, J.-W. Seo, J.-T. Jang, H.-T. Song, S. Kim, E.-J. Cho, H.-G. Yoon, J.-S. Suh, and J. Cheon, *Nat. Med.* **13**, 95 (2006).  
 [9] N.-H. Cho, T.-C. Cheong, H. M. Ji, H. W. Jun, S. J. Lee, D. Kim, J.-S. Yang, S. Kim, Y. K. Kim, and S.-Y. Seong, *Nat. Nanotechnol.* **6**, 675, (2011).  
 [10] C. B. Murray, D. J. Noms, and M. G. Bawendi, *J. Am. Chem. Soc.* **115**, 8706 (1993).  
 [11] V. K. La Mer, R. H. Dinegar, *J. Am. Chem. Soc.* **72**, 4847 (1950).  
 [12] Y. H. Li, T. Kouh, I.-B. Shim, and C. S. Kim, *J. Appl. Phys.* **111**, 07B544 (2012).  
 [13] M. Suto, Y. Hirota, H. Mamiya, A. Fujita, R. Kasuya, K. Tohji, and B. Jeyadevan, *J. Magn. Magn. Mater.* **321**, 1493 (2009).